

Joule Effect of Heat Transfer of Power-Law Fluid Along the Cylinder

Zaffer Elahi*, Walija Gul[†], Azeem Shahzad[‡]

*zaffer.elahi@uettaxila.edu.pk, Department of Mathematical Sciences, University of Engineering and Technology, Taxila -47050, Pakistan,

[†]22-ms-mth-3@students.uettaxila.edu.pk, Department of Mathematical Sciences, University of Engineering and Technology, Taxila -47050, Pakistan,

[‡]azeem.shahzad@uettaxila.edu.pk, Department of Mathematical Sciences, University of Engineering and Technology, Taxila-47050, Pakistan.

Abstract

The purpose of this research is to study the effect of heat transfer and flow of non-Newtonian power law fluids across a stretching cylinder in the presence of a magnetic field and joule heating effect. It specifically explores the influence of numerous emerging parameters on the heat distribution, including the unsteadiness parameter, the curvature parameter, the Eckert number, and the Prandtl parameter. Suitable similarity transformations are used to change the non-linear partial differential equations to ordinary differential equations. For the numerical solution, MATLAB software, by applying the built-in command `bvp4c` with `numeric`, is utilised. Results are proposed in the form of graphs and numerical tables. The behaviour of both pseudoplastic and dilatant fluid is compared.

Keywords: Non-Newtonian Fluid; Power Law Index; Joule Heating Effect; Boundary Layer.

Date of Submission: 06-05-2024

Date of acceptance: 18-05-2024

I. Introduction

The study of non-Newtonian fluids in fluid mechanics has proven difficult since there isn't a generic model that can adequately capture the variety of characteristics of these fluids. Consequently, a number of viscous rheology prototypes have been developed in an effort to mimic the dynamic patterns found in non-Newtonian fluids. These models are intended to enhance our knowledge of fluid dynamics. The most fundamental non-Newtonian fluid model that explains the behaviour of real non-Newtonian liquids is the Ostwald-de Waele liquid, often known as the power-law fluid. Shear thinning and shear thickening are the two categories under which non-Newtonian liquids are classified. Certain fluids, such as commercial carboxymethyl cellulose in water, cement rock in water, napalm in kerosene, lime in water, and Illinois yellow clay in water, are power law fluids among these non-Newtonian fluids. There are several industrial uses for boundary layer flow and heat transfer across a stretching cylinder. Numerous constitutive equations have been proposed to forecast the performance of non-Newtonian fluids in engineering and industry. Two and three-dimensional boundary layer equations have been developed by Schowalter *et al.* [1] for non-Newtonian fluids. Chen *et al.* [2] have researched momentum and heat transmission in a thin power-law fluid liquid sheet on an unsteady stretched surface. Patnana *et al.* [3] has conducted a numerical study on the forced convection heat transfer characteristics of a cylinder submerged in a streaming power-law fluid while maintaining a constant temperature in the two-dimensional unstable flow regime. For a considerable amount of time, researchers have been interested in studying heat transfer analysis in the setting of non-Newtonian fluid flowing driven by a non-linear boundary surface. Numerous fluids that are frequently found in the domains of engineering, science, and manufacturing, such as biological fluids, food items, cosmetics, particulate slurries, mixtures of multiple phases, artificial emollients, dyes, and different polymerized liquids, among others, display characteristics that differ from the conventional Newton's law of viscosity. The presence of regular stresses, viscosity, and unsteady elastic effects, which point to the complex behaviour of these liquids, demonstrate their non-Newtonian character. In the presence of a non-uniform heat source/sink, Abel *et al.* [4] investigated the flow of a power-law fluid caused by a linearly stretching sheet and heat transfer characteristics utilising varying thermal conductivity. It is believed that temperature has a linear relationship with thermal conductivity. Hassanien *et al.* [5] have published a boundary layer analysis for the flow and heat transfer problem from a power-law fluid to a continuous stretched sheet with a variable wall temperature.

Heat transfer in fluids has a wide range of industrial uses, from straightforward static designs to sophisticated

multi-loop systems that carry out many tasks in a production process. There are various variations in the design and application of processes that employ heat transfer fluids, which accounts for the wide range of businesses that employ this approach. Dhiman *et al.* [6] have studied numerically forced convection heat transfer in power-law fluids from a heated square cylinder. In the presence of thermal radiation and a constant heat flow, Megahed [7] investigated the heat transfer characteristics of a non-Newtonian power law fluid by considering a non-linearly impermeable stretched vertical sheet. He noticed that the skin friction coefficient decreases when the power-law index, mixed convection, and radiation parameters are increased, whereas the local Nusselt number rises as the Prandtl number is increased. In a non-Newtonian power law fluid, Howell *et al.* [8] investigate the momentum and heat transfer taking place in the laminar boundary layer over a two dimensional surface that is stretching. A vertically stretching cylinder was explored by Naseer *et al.* [9] in terms of its axial direction boundary layer flow and heat transfer of Power Law fluid.

The physical process by which thermal energy is produced when current flows through an electrical conductor is known as joule heating. The word “heating” refers to the increase in conductor material temperature that results from this thermal energy. In accordance with the energy conservation concept, joule heating may be understood as a conversion between electrical energy and thermal energy. Joule heating is a widely used technique in household, industrial, and transportation equipment, like in incandescent light bulbs, resistance ovens, industrial electric ovens, and to remove moisture or cure paint. Ahmed *et al.* [10] numerically analyse the effects of viscous dissipation and joule heating on the forced convection heat transfer rate of electrically conducting magnetohydrodynamic (MHD) power law fluid flow through an annular duct. Furthermore, Shit *et al.* [11] developed a mathematical model to study the electro-osmotic flow and heat transfer of bio-fluids in a micro-channel in the presence of joule heating effects.

Regarding the situation, we employed convective boundary conditions and the joule heating effect, and we are analysing the flow and heat transfer rate of a power-law fluid across an unsteady stretched cylinder in a horizontal direction. This has never been documented or investigated before.

II. Mathematical Formulation

We have considered an unsteady, two-dimensional flow of an incompressible, electrically conducting, power law fluid over a stretched cylinder. The velocity at which the cylinder is stretched corresponds to its length. Along the r -axis, a uniform magnetic field is applied. The stretching velocity of the cylinder, magnetic field and temperature of the fluid are expressed as

$$U = \frac{bz}{(1 - \alpha t)}, \quad B = \frac{B_o}{(1 - \alpha t)}, \quad T = T_\infty + \frac{cz}{(1 - \alpha t)}\theta(\eta)$$

where b and c are the dimensional constants, z is the characteristic length, and T is the temperature of the fluid. The governing equations that clarify the conservation of mass, momentum, and energy in the presence of the Joule heating effect under the boundary-layer approximation are expressed as follows [12]

$$\frac{\partial u}{\partial r} + \frac{u}{r} + \frac{\partial w}{\partial z} = 0, \tag{1}$$

$$\rho \left[\frac{\partial w}{\partial t} + u \frac{\partial w}{\partial r} + w \frac{\partial w}{\partial z} \right] - \frac{1}{r} \frac{\partial}{\partial r} \left(rk \left| \frac{\partial w}{\partial r} \right|^{n-1} \frac{\partial w}{\partial r} \right) + \sigma w B^2 = 0, \tag{2}$$

$$\rho C_p \left[\frac{\partial T}{\partial t} + u \frac{\partial T}{\partial r} + w \frac{\partial T}{\partial z} \right] - k \left(\frac{-\partial w}{\partial r} \right)^{n+1} - k_* \left| \frac{\partial T}{\partial r} \right|^{n-1} \left(\frac{\partial^2 T}{\partial r^2} + \frac{1}{r} \frac{\partial T}{\partial r} \right) - \sigma w^2 B^2 = 0, \quad (3)$$

with boundary conditions [13]

$$\begin{aligned} \text{At } r = R \quad u = 0, \quad w = U, \quad T = T_w \\ \text{as } r \rightarrow \infty \quad w \rightarrow 0, \quad T \rightarrow T_\infty \end{aligned} \quad (4)$$

where σ is the electric conductivity of the medium, C_p is the specific heat constant, n is the power-law index, and σ is the fluid density. Employing local similarity transformations, as [14]

$$\begin{aligned} \eta = \frac{r^2 - R^2}{2zR} Re^{\frac{1}{n+1}}, \quad Re = \frac{z^n U^{2-n}}{\frac{k}{\rho}}, \\ \psi = zRU Re^{\frac{-1}{n+1}} f(\eta), \quad \theta(\eta) = \frac{T - T_\infty}{T_w - T_\infty} \end{aligned} \quad (5)$$

where η denotes the dimensionless local similarity variable and ψ the stream function such that

$$u = -\frac{1}{r} \frac{\partial \psi}{\partial z}, \quad \text{and} \quad w = \frac{1}{r} \frac{\partial \psi}{\partial r} \quad (6)$$

In consideration of the previous transformations, the incompressibility condition (1) is automatically satisfied, while eqs. (2)–(4) are reduced to:

$$\begin{aligned} \left[(1+n) C (1+2\eta C)^{\frac{n-1}{2}} (-f'')^n \right] - (n) \left[(1+2\eta C)^{\frac{n+1}{2}} (-f'')^{n-1} f''' \right] - \left(\frac{2n}{n+1} \right) f f'' \\ + [f']^2 + A \left[f' + \eta \left(\frac{2-n}{n+1} \right) f'' \right] + M f' = 0, \end{aligned} \quad (7)$$

$$\begin{aligned} Pr E_c \left[(1+2\eta C)^{\frac{n+1}{2}} (-f'')^{n+1} \right] - Pr A \left[\theta + \left(\frac{2-n}{n+1} \right) \theta' \eta \right] - \left[2 C (1+2\eta C)^{\frac{n-1}{2}} (-\theta)^n \right] \\ - Pr \left[\theta f' + \left(\frac{2n}{n+1} \right) \theta' f \right] + \left[(1+2\eta C)^{\frac{n+1}{2}} (-\theta')^{n-1} \theta'' \right] + Pr M E_c (f')^2 = 0. \end{aligned} \quad (8)$$

$$f(0) = 0, \quad f'(0) = 1, \quad \theta(0) = 1, \quad \text{at } \eta = 0,$$

$$f'(\eta) \rightarrow 0, \quad \theta(\eta) \rightarrow 0 \quad \text{as } \eta \rightarrow \infty. \quad (9)$$

where prime denotes differentiation with respect to η , A stands for the unsteadiness parameter, Pr is the Prandtl number, E_c is the Eckert number, M is magnetic parameter, and C is the curvature parameter defined as

$$A = \frac{\alpha}{b}, \quad Pr = k k_*^{-1} C_p b^{n-1} c^{1-n}, \quad E_c = \frac{U^2}{C_p (T_w - T_\infty)}, \quad M = \frac{\sigma B B_0}{\rho b}, \quad C = \frac{z}{R} Re^{\frac{-1}{n+1}} \quad (10)$$

The expression for the local skin friction coefficient and the local Nusselt number is given

$$C_f = \frac{2 \tau_w}{\rho U^2}, \quad \text{and} \quad Nu = \frac{z q_w}{k (T_w - T_\infty)} \quad (11)$$

where

$$\tau_w = k \left(\frac{\partial w}{\partial r} \right)_{r=R}^n, \text{ and } q_w = -k \left(\frac{\partial T}{\partial r} \right)_{r=R}$$

In view of eq. (5), the dimensionless forms of the local skin friction coefficient and the local Nusselt number can be obtained

$$\frac{1}{2} C_f Re^{\frac{1}{n+1}} = - \left[-f''(0) \right]^n, \quad \text{and} \quad Nu Re^{\frac{-1}{n+1}} = -\theta'(0). \quad (12)$$

III. Results and Discussion

In this paper, we have used the BVP4C solver [15, 16] to solve the boundary value problems numerically. The solutions are depicted through graphs and tables for different parameters. The magnetic parameter, the Prandtl number, the curvature parameter, the unsteadiness parameter, and the Eckert number are being studied. Our main focus is to analyse the behaviour of these physical parameters. Tables 1 and 2 contain calculated values for the Nusselt number and skin friction coefficient, while figures display numerical data graphically. In Figure 1 we analyse the effect of the Prandtl number on the temperature profile. The increase in Pr number causes a decrease in temperature of a power law fluid at a specified distance. On the other hand, an increase in Pr causes an increase in the fluid viscosity. This trend is slower for the shear-thickening fluid and faster for the shear-thinning fluid. This implies that an increase in Prandtl number is accompanied by a decrease in thermal conductivity, which means that the fluid transfers more heat effectively through convection. Thereby, the thickness of the thermal boundary layer gets reduced.

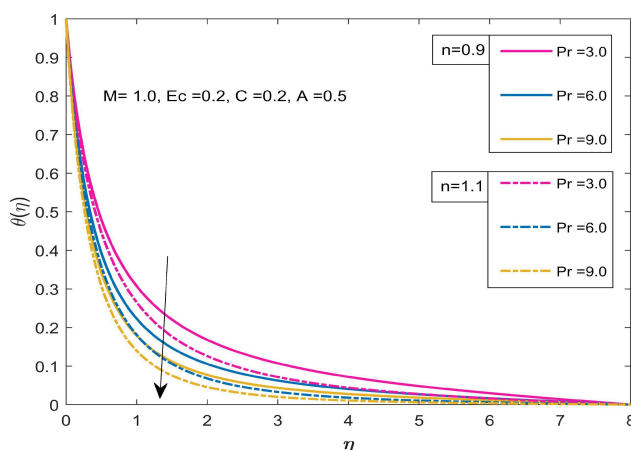


Figure 1: Variation of Pr on heat transfer

The distinction in the fluid temperature owing to the alteration of Eckert number Ec has been illustrated in Figure 2. The figure shows that, with an increased value of Ec, the fluid temperature intensifies. This happens because heat is produced in the fluid as the value of Ec increases due to frictional heating. Physically, Eckert number is the ratio of kinetic energy to the specific enthalpy difference between wall and fluid. Therefore, an increase in Eckert number causes the transformation of kinetic energy into internal energy by work that is done against the viscous fluid stresses. Due to this, increasing Ec enhances the temperature of the fluid.

In Figure 3, the influence of magnetic field M on the temperature profile of the fluid has been displayed. From the figure, it is noticeable that the temperature increases with a rise in the magnetic field parameter M. Physically, when M is increased, an opposing force (Lorentz force) that retards the flow motion will be produced in the fluid. In fact, the presence of a magnetic field decelerates velocity and consecutively persuades the temperature field, which increases the temperature profiles.

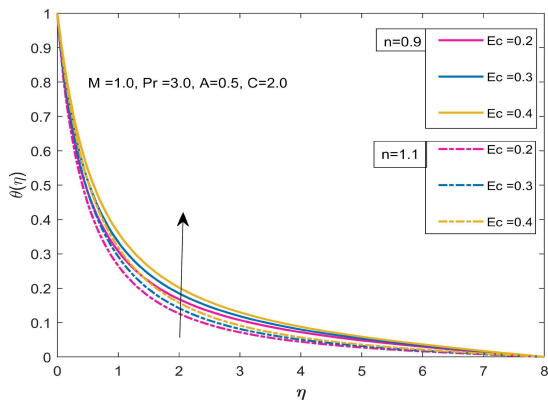


Figure 2: Variation of Ec on heat transfer

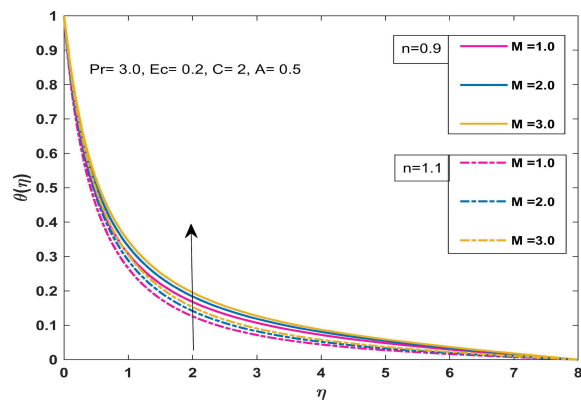


Figure 3: Variation of M on heat transfer

As the unsteadiness parameter increases, the temperature gradually decreases, as shown in Figure 4. Physically, the value of the unsteadiness parameter grows, and the thickness of the thermal boundary layer decreases, which results in a decline in the temperature profile. The influence of the curvature parameter A, on the temperature profile is presented in Figure 5. A smaller value of the curvature parameter A indicates that the cylinder has a larger radius. In the case of a cylinder, as the curvature increases, the surface area exposed to the surrounding fluid also increases. This enhances convective heat transfer, as there's more surface area for the fluid to exchange heat with. Additionally, the flow behaviour near the surface can change with increasing curvature, affecting the heat transfer coefficient. In this case, as shown in Figure 5, higher curvature leads to increased turbulence near the surface, which enhances heat transfer through convective mechanisms.

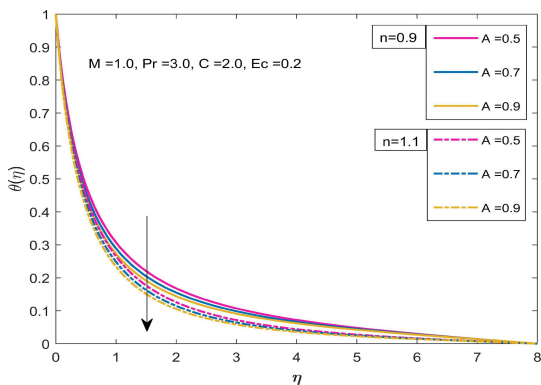


Figure 4: Variation of A on heat transfer

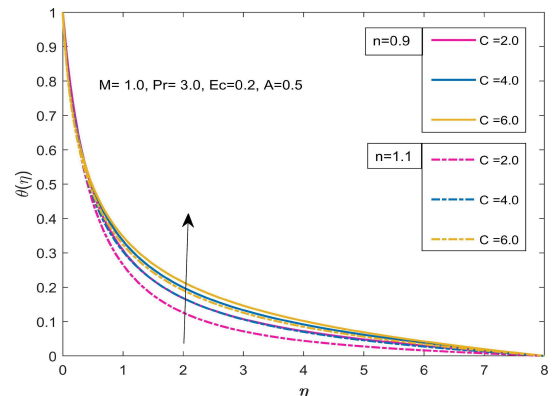


Figure 5: Variation of C on heat transfer

Table 1 shows the numerical value of skin friction for pseudoplastic fluid ($n < 1$) and dilatant fluid ($n > 1$). It is observed that increasing magnetic number increases the skin friction coefficient. Similar results are observed for the varying values of the curvature parameter and the unsteadiness parameter.

Finally, Table 2 presented a full description of the behaviour of relevant physical quantities, such as the local Nusselt number with changes in the power-law index parameter n , the Eckert number Ec , the curvature parameter C , and the Prandtl number Pr , respectively. It can be seen that increasing the index parameter n results in an increase in the Nusselt number for Prandtl number Pr , curvature parameter C , and unsteadiness parameter A . The local Nusselt number decreases as Eckert varies, and similar decreasing behaviour is observed for the magnetic parameter. Additionally, an increase in the Prandtl number leads to an increase in the local Nusselt number. This is because a fluid with a higher Prandtl number has a higher heat capacity and hence increases heat transport.

Table 1: Analysis of Skin Friction Coefficient

Non- <i>M</i>	Dimensional <i>C</i>	Variables			Skin Friction	
		<i>A</i>	<i>n = 0.9</i>	<i>n = 1.1</i>		
1	2	0.5	2.5207	2.1788		
2			2.8816	2.4712		
3			3.1890	2.7167		
1	2		2.5207	2.1788		
	4		3.3278	2.7701		
	6		4.0930	3.3226		
	2	0.5	2.5207	2.1788		
		0.7	2.5772	2.2288		
		0.9	2.6322	2.2771		

Table 2: Analysis of Local Nusselt Parameter

Non- <i>M</i>	Dimensional <i>Pr</i>	Variables				Skin Friction	
		<i>C</i>	<i>Ec</i>	<i>A</i>	<i>n = 0.9</i>	<i>n = 1.1</i>	
1	3	2	0.2	0.5	2.1153	2.2552	
2					1.8616	2.0102	
3					1.6528	1.8021	
1	3				2.1153	2.2552	
	6				2.6082	2.7693	
	9				2.9459	3.1209	
	3	2			2.1153	2.2552	
		4			2.5559	2.7358	
		6			2.9723	3.1870	
		2	0.2		2.1153	2.2552	
			0.3		1.7727	1.9467	
			0.4		1.4354	1.6343	
			0.2	0.5	2.1153	2.2552	
			0.7		2.2548	2.3808	
			0.9		2.3840	2.4964	

IV. Main Findings

This paper deals with the study of flow and heat transfer enhancement in the power law fluid model while utilising the Joule heating effect. The numerical simulations of the proposed model are completed using BVP4C solver in MATLAB package and interpreted in the following lines, as

- The growing values of curvature and Eckert number give rise to temperature profile, while the reverse trend is observed against the Prandtl number.
- On varying the Eckert number, the Nusselt number decreases, but the opposite trend is found in the Prandtl number.
- Pseudoplastic fluid acquires more wall shear stress as compared to dilatant in the context of skin friction coefficient.
- It should be noted that the Nusselt number is improving for the power law index n .
- The skin friction coefficient extends with increasing estimations of the magnetic parameter, curvature parameter, and the unsteadiness parameter.

References

- [1]. W. R. Schowalter, "The application of boundary-layer theory to power-law pseudo-plastic fluids: Similar solutions," *AIChE Journal*, vol. 6, no. 1, pp. 24–28, 1960.
- [2]. C.-H. Chen, "Heat transfer in a power-law fluid film over a unsteady stretching sheet,"
- [3]. *Heat and Mass transfer*, vol. 39, no. 8, pp. 791–796, 2003.
- [4]. V. K. Patnana, R. P. Bharti, and R. P. Chhabra, "Two-dimensional unsteady forced convection heat transfer in power-law fluids from a cylinder," *International Journal of Heat and Mass Transfer*, vol. 53, no. 19-20, pp. 4152–4167, 2010.
- [5]. M. S. Abel, P. Datti, and N. Mahesha, "Flow and heat transfer in a power-law fluid over a stretching sheet with variable thermal conductivity and non-uniform heat source," *International Journal of Heat and Mass Transfer*, vol. 52, no. 11-12, pp. 2902–2913, 2009.
- [6]. I. Hassanien, A. Abdullah, and R. Gorla, "Flow and heat transfer in a power-law fluid over a nonisothermal stretching sheet," *Mathematical and Computer Modelling*, vol. 28, no. 9, pp. 105–116, 1998.
- [7]. A. Dhiman, R. Chhabra, and V. Eswaran, "Heat transfer to power-law fluids from a heated square cylinder," *Numerical Heat*

- Transfer, Part A: Applications, vol. 52, no. 2, pp. 185–201, 2007.
- [8]. A. M. Megahed, “Flow and heat transfer of a non-newtonian power-law fluid over a non-linearly stretching vertical surface with heat flux and thermal radiation,” *Meccanica*, vol. 50, no. 7, pp. 1693–1700, 2015.
- [9]. T. Howell, D. Jeng, and K. De Witt, “Momentum and heat transfer on a continuous moving surface in a power law fluid,” *International Journal of Heat and Mass Transfer*, vol. 40, no. 8, pp. 1853–1861, 1997.
- [10]. M. Naseer, M. Malik, and A. Rehman, “Numerical study of convective heat transfer on the power law fluid over a vertical exponentially stretching cylinder,” *Applied and Computational Mathematics*, vol. 4, no. 5, pp. 346–350, 2015.
- [11]. F. Ahmed, M. Iqbal, and N. S. Akbar, “Viscous dissipation and joule heating effects on forced convection power law fluid flow through annular duct,” *Proceedings of the Institution of Mechanical Engineers, Part C: Journal of Mechanical Engineering Science*, vol. 235, no. 21, pp. 5858–5865, 2021.
- [12]. G. Shit, A. Mondal, A. Sinha, and P. Kundu, “Electro-osmotic flow of power-law fluid and heat transfer in a micro-channel with effects of joule heating and thermal radiation,” *Physica A: Statistical Mechanics and its Applications*, vol. 462, pp. 1040–1057, 2016.
- [13]. K. Vajravelu, K. Prasad, S. Santhi, and V. Umesh, “Fluid flow and heat transfer over a permeable stretching cylinder,” *Journal of Applied Fluid Mechanics*, vol. 7, no. 1, pp. 111–120, 2014.
- [14]. Z. Elahi, M. Khalid, and A. Shahzad, “Analysis of heat transfer of power-law fluid along a vertical stretching cylinder,” *Innovative Journal of Mathematics (IJM)*, vol. 1, no. 3, pp. 1–11, 2022.
- [15]. Hashim, M. Khan, and A. Saleh Alshomrani, “Characteristics of melting heat transfer during flow of carreau fluid induced by a stretching cylinder,” *The European Physical Journal E*, vol. 40, pp. 1–9, 2017.
- [16]. L. F. Shampine, J. Kierzenka, M. W. Reichelt, et al., “Solving boundary value problems for ordinary differential equations in matlab with bvp4c,” *Tutorial notes*, vol. 2000, pp. 1–27, 2000.
- [17]. L. F. Shampine, “Singular boundary value problems for odes,” *Applied Mathematics and Computation*, vol. 138, no. 1, pp. 99–112, 2003.